The Journal of Experimental Biology 214, 1560-1570

doi:10.1242/jeb.053702

RESEARCH ARTICLE

Atypical properties of release and short-term depression at a specialized nicotinic synapse in the Mauthner cell network

Simon Gelman*, Charlotte L. Grove and Donald S. Faber

Dominick P. Purpura Department of Neuroscience, Albert Einstein College of Medicine of Yeshiva University, Bronx, NY 10461, USA

*Author for correspondence (s.gelman@einstein.yu.edu)

Accepted 20 January 2011

SUMMARY

Many synapses exhibit temporally complex forms of activity-dependent short-term synaptic plasticity. The diversity of these phenomena reflects the evolutionary specialization of synapses within networks. We examined the properties of transmission and plasticity, *in vivo*, at an identified, specialized axo-axonic nicotinic synapse between the goldfish Mauthner cell and one of its targets, the cranial relay neuron (CRN), using intracellular paired recordings and low frequency (0.33–2 Hz) train stimulations. Depression of successive excitatory postsynaptic potentials (EPSPs), which dominates short-term plasticity, had two components. A fast component reduced the amplitude of $EPSP_2$, to less than 50% of $EPSP_1$. A slow component produced an additional 10–30% of amplitude reduction and developed with a time constant of tens of seconds. The latencies of the later depressed responses were ~0.1 ms longer than that of $EPSP_1$, suggesting a reduced release probability. The Ca^{2+} chelators EGTA and BAPTA, injected presynaptically, reduced all EPSPs and slowed development of the second component of depression. Interestingly, spike broadening, produced by injecting K^+ channel blockers, reduced release, but accelerated the kinetics of the slow component. Finally, Ba^{2+} in the external medium enhanced release, and reduced the first component and slowed the development of the second component of depression. Taken together, these last two results, which are in contrast to observations at other synapses, and the two-component depression suggest atypical release properties at the output synapses of the Mauthner cell, which triggers an escape behavior. We suggest that the second component of depression provides an additional safety factor to prevent repetitive firing of the CRN.

Key words: latency, calcium buffers, calcium domains, potassium channel blockers, barium, escape.

INTRODUCTION

The diversity of animal behaviors partly originates in the structural and functional variations of neurons, including their synaptic connections, which comprise neuronal networks. Synapses between neurons differ in their presynaptic and postsynaptic morphology, neurotransmitter release and postsynaptic responsiveness. Differences in dynamic properties include, among others, release rate, calcium sensitivity and activity-dependent plasticity.

Repetitive activity leads to short- and long-term changes in the efficacy of synaptic transmission (Kandel et al., 2000). Synaptic plasticity, on a time scale of milliseconds to minutes, is computationally important (Abbott et al., 1997) and is implicated in processes such as adaptation, sensitization, detection of change and signal filtering (Castellucci and Kandel, 1974; Fortune and Rose, 2000; MacLeod et al., 2007). Presynaptic forms of short-term depression are attributed to several processes with different kinetics, classified as very fast (<500 ms), fast (~6 s) and slow (tens of seconds to minutes) (Betz, 1970; Stevens and Wesseling, 1999; Kalkstein and Magleby, 2004; Garcia-Perez et al., 2008). Additionally, superimposed synaptic facilitation, masked by depression, may influence the observed kinetics of activity-dependent synaptic plasticity. Interactions between various forms of plasticity are not well understood at the phenomenological and mechanistic levels.

Presumably, evolutionary modification of morphology and release, and synaptic plasticity, sculpted synapses to optimally perform their functions. Such modifications can best be studied using specialized synapses, especially if the associated networks and behaviors are simple and well understood. Thus, studying release and its plasticity at such synapses may lead to a better understanding of the evolutionary synaptic adaptations underlying behavior. Additionally, investigation of the kinetics of short-term plasticity and its mechanisms at identified and specialized synapses in defined microcircuits is essential in understanding the functional role of this plasticity.

In this study, we explored release and its dynamics at output synapses of the Mauthner (M-) cell in the teleost brainstem escape network (Gahtan et al., 2002). In goldfish, one M-cell action potential activates downstream connections with a high safety factor and reliably triggers an escape response (Faber and Korn, 1978). The first relay in the output pathway, the excitatory, nicotinic axo-axonic synapses between the M-cell axon collaterals and cranial relay neurons (CRNs, a heterogeneous group of interneurons), exhibits a marked depression (Hackett et al., 1989). Previous work indicates that this is a highly specialized junction with an unusually short synaptic delay (reviewed in Lin and Faber, 2002) and a high safety factor for impulse transmission (Hackett and Faber, 1983). Also, it has been used to demonstrate a form of paired pulse depression that is due to a reduction in the release probability, lasting ~100–300 ms (Waldeck et al., 2000). Here, we describe additional properties of depression; namely, a two-component depression during lower frequency (0.33–2 Hz) stimulation, the kinetics of which are Ca^{2+} dependent, and show that increasing M-axon spike duration

anomalously reduces transmitter release. Additionally, these synapses uniquely exhibit Ba^{2+}-induced synaptic enhancement, which may be related to an atypical calcium sensor for release. We suggest that these specializations are part of a repertoire of cellular and synaptic adaptations in the M-cell network that support optimization of the escape reflex.

MATERIALS AND METHODS

Animals

Adult goldfish, *Carassius auratus* (Linnaeus), were used for all experiments. Fish were housed in aquaria containing conditioned water at 17–18°C (Szabó et al., 2006). All procedures complied with the Albert Einstein College of Medicine IACUC guidelines.

Experimental preparation

Surgical procedures followed those established for studying the goldfish M-cell and its associated network (Faber and Korn, 1978; Waldeck et al., 2000). Goldfish were anesthetized in and continuously perfused through the mouth with conditioned water (6±2°C), containing 50 mg l^{-1} MS-222 (general anesthetic, ethyl 3-aminobenzoate methanesulfonate salt, Sigma-Aldrich, St Louis, MO, USA). The brain was continuously superfused with a standard goldfish extracellular solution [mmol l^{-1}: 124.0 NaCl, 5.0 KCl, 2.8 $Na_2H_2PO_4$ (monohydrate), 0.91 $MgCl_2$ (hexahydrate), 20 Hepes, 1.63 $CaCl_2$ (dihydrate), 3.0 dextrose]. Animals were immobilized with an intramuscular injection of *d*-tubocurarine chloride (~0.2–0.5 ml of a 0.3 mg ml^{-1} solution; Abbott Laboratories, North Chicago, IL, USA).

Electrophysiological recordings

Paired intracellular recordings were made in current-clamp mode with sharp micropipette electrodes (electrode resistances: M-axon, 5–10 MΩ; CRN, 10–18 MΩ) using an Axoprobe-1A microelectrode amplifier with cross-neutralization (Axon Instruments, Foster City, CA, USA). For control experiments, M-axon and CRN electrodes were filled with a 2.5 mol l^{-1} KCl solution (pH 7.2; buffered with 10 mmol l^{-1} Hepes). CRN electrodes also contained QX314 (70 mmol l^{-1}; Sigma-Aldrich). QX314, a quaternary lidocaine derivative, blocks voltage-sensitive Na^+ conductance (Strichartz, 1973; Connors and Prince, 1982) and was used to block postsynaptic action potentials (Fig. 1) (Grove, 2008). M-axons were activated intracellularly by short depolarizing current pulses (10–15 nA, 10–30 ms), which generated single action potentials. Antidromic stimulation of the M-axons was accomplished with a bipolar electrode positioned on the exposed caudal spinal column. Stimulus timing/duration was controlled with a Master-8 stimulator (A.M.P.I., Jerusalem, Israel). In each experiment, trains of 100–200 suprathreshold intracellular stimulations of the M-axons, delivered at 0.33–2 Hz, were separated by 1 min intervals. Each stimulus in a train produced an M-cell action potential, which evoked an excitatory postsynaptic potential (EPSP). The EPSPs were then averaged between trains of the same frequency and different M-axon/CRN pairs. When evoked release was modified pharmacologically, the first 2–5 control trains were followed by 3–10 experimental trains. Each experimental train was preceded by 1–2 min of iontophoretic/pressure injection of calcium chelators or potassium channel blockers (see 'Pharmacological manipulations'). In experiments that determined the time course of recovery from depression, the M-axon was stimulated with conditioning trains of 50 stimuli (2 Hz) followed by a test stimulus, 1, 2, 5, 10, 20, 50 or 100 s later. The interval between the test stimulus and the next conditioning train was >60 s, which was determined to be sufficient for complete recovery from depression.

The M-axons were identified visually with the aid of a stereomicroscope and electrophysiologically (Fig. 1A,B). The CRNs, which synapse with the M-axon collaterals every 100–200 μm (Funch et al., 1984), were identified electrophysiologically (Fig. 1A,B), based on the EPSP waveform and short latency (Hackett and Faber, 1983; Hackett et al., 1989; Waldeck et al., 2000).

Pharmacological manipulations

The calcium buffers BAPTA and EGTA (10 or 100 mmol l^{-1} in 2.5 mol l^{-1} KCl solution, pH 7.2) were pressure injected into the M-axon, using a custom-made injection system. In some experiments, 100 mmol l^{-1} EGTA solution was buffered with 40 mmol l^{-1} $CaCl_2$ to achieve a nominal free [Ca^{2+}] in the pipette of 100 nmol l^{-1}, as calculated with the web-based program WEBMAXC EXTENDED (Patton et al., 2004). The M-axon action potential duration was

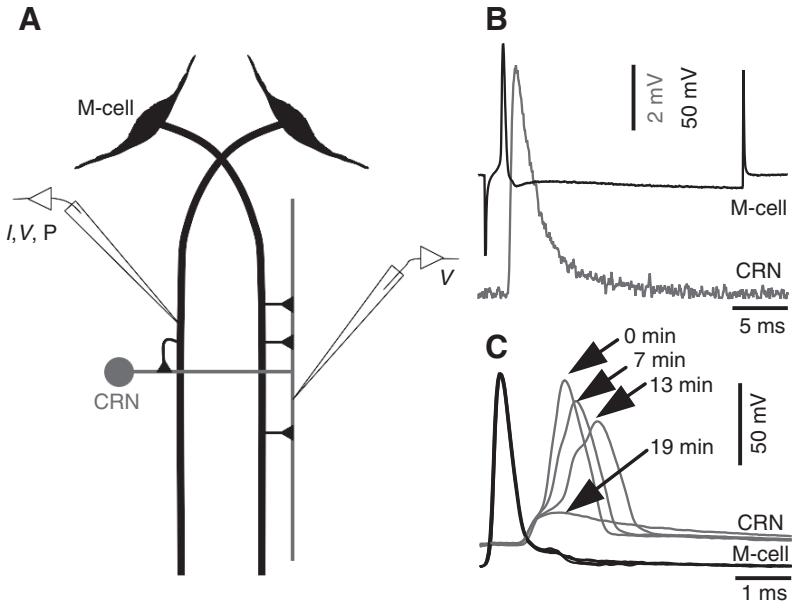

Fig. 1. (A) A diagram depicting the Mauthner (M-) cell network and recording arrangement. The M-cell electrode (left) was used to inject depolarizing current (*I*), record voltage (*V*), and pressure inject (P) various compounds. The cranial relay neuron (CRN) electrode (right) was used to record excitatory postsynaptic potentials (EPSPs) and contained QX314 to block voltage-sensitive Na^+ current. (B) An example of the M-cell spike (black) and evoked CRN EPSP (gray). (C) An example of the QX314 effect (note the block of the rising phase of the spike at different spike-generating zones).

increased by iontophoretic and pressure injection of a mixture of the K^+-channel blockers tetraethylammonium chloride (TEA, 2 mol l^{-1}) and 4-aminopyridine (4-AP, 0.1 mol l^{-1}; Sigma-Aldrich) in 1 mol l^{-1} KCl solution (pH 7.2) (Kaars and Faber, 1981). In some experiments, $CaCl_2$ in the control extracellular solution was replaced with an equimolar amount of $BaCl_2$.

Data acquisition and analysis

Data were digitized at 33 kHz with an NI DAQ card (PCIe-6251, National Instruments, Austin, TX, USA) and collected with a G5 Macintosh computer, using custom-designed acquisition software. Analysis was performed using Igor Pro (WaveMetrics, Portland, OR, USA) and GraphPad Prism v.5 (GraphPad Software, La Jolla, CA, USA). EPSP amplitude data were fitted with exponential functions using a non-linear, least-squares regression analysis.

RESULTS

Kinetics of depression

We characterized the kinetics of activity-dependent short-term plasticity at the M-axon to CRN connection, using the notation $EPSP_X$ to denote the Xth response in a train (the steady-state EPSP is denoted as $EPSP_{SS}$). When the M-axon was repetitively stimulated at low frequency, there was a pronounced depression of the amplitude of $EPSP_2$ in the train, and the depression increased progressively to reach a steady-state level in ~50–100 s (Fig. 2). Additionally, there appeared to be an abrupt change in the rate of depression (Fig. 2A,B). As may be expected, the magnitudes of both the initial and steady-state depression were greatest at the highest stimulation frequency. The first component of depression was rapid and corresponded to a greater than 50% decrease in EPSP amplitude relative to $EPSP_1$ (Fig. 2C). The second component developed over tens of seconds and accounted for an additional 10–30% amplitude reduction (Fig. 2C). In order to quantify the kinetics of this depression, we attempted to fit various composite exponential functions to the data. However, because of the very fast and profound initial depression after the first stimulus, most of the fits were unsatisfactory. Conversely, the time course of the depression from $EPSP_2$ to $EPSP_{SS}$ (the steady-state amplitude) could be described by an exponential decay with one time constant (Fig. 2C). That is, a single exponential function:

$$EPSP(t) = D^*_{slow}\, e^{(-t/\tau)} + EPSP_{SS} \quad (1)$$

[where t=0 corresponds to the time of $EPSP_2$, $EPSP(t)$ is the EPSP amplitude at time t, D^*_{slow} is the difference between the maximal EPSP in the fitted range and $EPSP_{SS}$, and τ is the time constant in seconds] provided a satisfactory fit of the averaged data (R^2=0.9524). The fitted parameters, τ and D^*_{slow} were 39.8 s and 0.22 (95% confidence intervals: 36.3–44.17 s and 0.21–0.22), respectively. To estimate the relative contributions of different components of depression in terms of magnitude, we subdivided the total or steady-state depression, D_{total}, into the fast, D_{fast}, and slow, D_{slow}, components (Fig. 2C). For a 1 Hz stimulation frequency, D_{total} averaged 0.80±0.02, D_{fast} averaged 0.56±0.05 and D_{slow} averaged 0.24±0.04 (means ± s.e.m.; N=19 pairs; Fig. 2D). Thus, the data indicate that under our experimental conditions the depression produced by the first stimulus in a train accounts for ~70% of the total depression and that the development of subsequent depression is one or two orders of magnitude slower. This observation leads us to suggest that there is a change in release properties after the first stimulus and that the total depression consists of a fast and slow component.

Next, we investigated the dependency of the fast and slow components of depression on stimulation frequency. For different frequencies, single exponential extrapolations from the decay in the first two EPSPs highlight the difference between the apparent initial time course and that of the fit to the slow component (Fig. 3A–D). Depression of EPSP amplitude starting from $EPSP_2$ or $EPSP_3$ follows an exponential time course (Fig. 3A–D). For these data sets, the estimated fast time constants (τ_{fast}) were 1.33 s (0.33 Hz), 1.62 s (0.67 Hz), 0.51 s (1.0 Hz) and 0.41 s (2.0 Hz). The slow time constants (τ_{slow}) were 90.90 s (0.33 Hz), 42.30 s (0.67 Hz), 32.50 s (1.0 Hz) and 7.28 s (2.0 Hz). τ_{fast} decreased linearly and τ_{slow} decreased

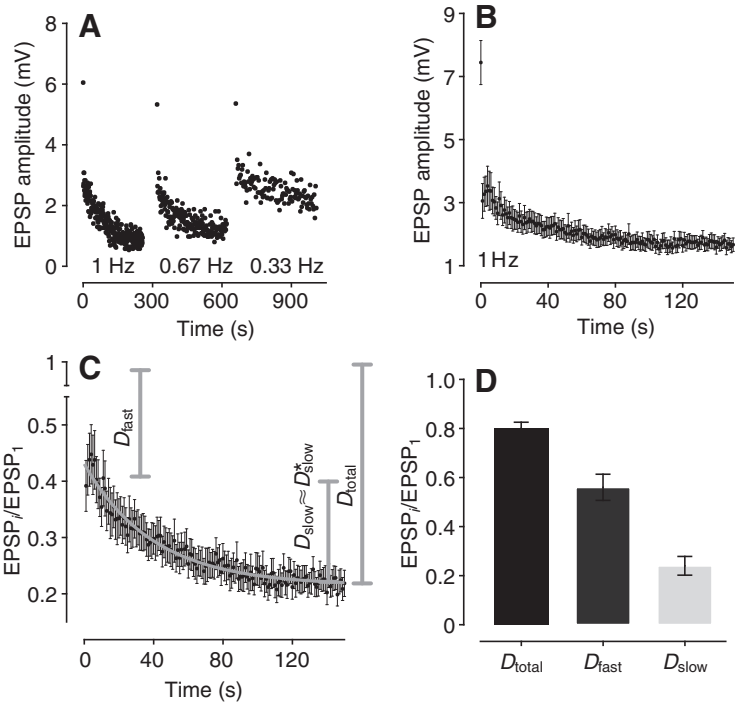

Fig. 2. (A) An example of EPSP amplitude depression. The M-cell axon was repetitively stimulated with three trains of stimuli, delivered at 1, 0.67 and 0.33 Hz. Each train was separated by a 1 min rest interval. Amplitudes of the successive EPSPs are plotted in each case. (B) Means of successive EPSP amplitudes during a 1 Hz stimulus train (successive data points represent means of the successive EPSPs in 1 Hz trains from N=19 M-axon/CRN pairs, ±s.e.m.). (C) Normalized data (same data as in B; $EPSP_1$ is omitted). Vertical lines depict the total (D_{total}), fast (D_{fast}) and slow (D_{slow}) components of depression. Total or steady-state depression was defined as D_{total}=1–$EPSP_{SS}$/$EPSP_1$, where $EPSP_{SS}$ is the mean amplitude of the last 20 EPSPs in a train, the fast component as D_{fast}=1–$EPSP_{2...6}$/$EPSP_1$, where $EPSP_{2...6}$ is the mean amplitude of five consecutive EPSPs starting from $EPSP_2$, and the slow component as D_{slow}=($EPSP_{2...6}$–$EPSP_{SS}$)/$EPSP_1$. D_{slow}, so defined, was always approximately equal to D^*_{slow}, obtained from an exponential fit (Eqn 1, see Results). The gray curve is a single exponential fit with τ=39.8 s and D^*_{slow}=0.22 (Eqn 1, see Results). (D) Summary data of the D_{total}, D_{fast} and D_{slow} components of depression for the same data as in B and C.

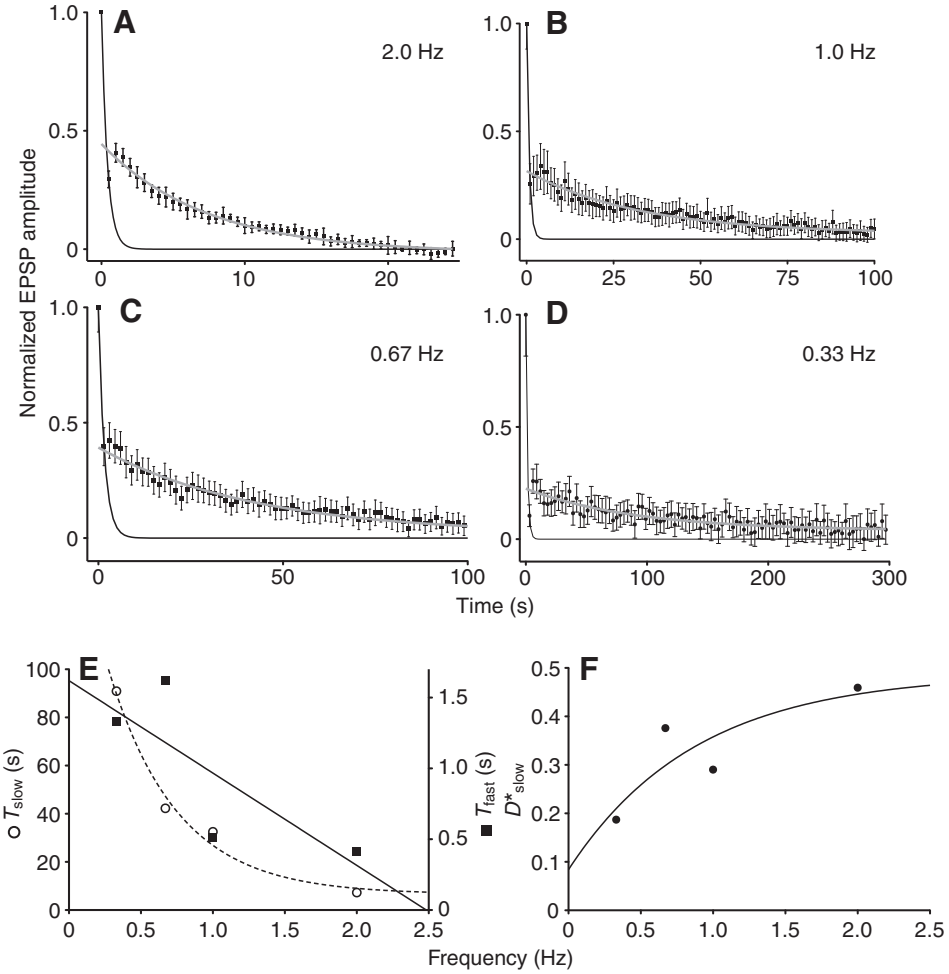

Fig. 3. (A–D) Scaled and normalized data for trains of stimuli delivered at different frequencies (means ± s.e.m.; N=6, 19, 42 and 16 M-axon/CRN pairs for A, B, C and D, respectively). Black curves are mono-exponential fits to the first and second points; gray curves are fits to the data starting from the third point ($EPSP_3$). (E) Plot illustrating the dependence of the slow time constant τ_{slow} (open circles, left y-axis) and the fast time constant τ_{fast} (filled squares, right y-axis) on the stimulation frequency. Note that τ_{slow} decays exponentially (fitted curve is $y=166.7e^{(-x/0.48)}$; R^2=0.9834, dashed curve) and τ_{fast} decreases linearly with increasing frequency (fitted line is $y=-0.65x+1.62$; R^2=0.6147, solid line). (F) The dependence of D^*_{slow} on the stimulation frequency was approximately exponential (fitted curve is $y=0.49-0.41e^{(-x/0.88)}$; R^2=0.7256).

exponentially as a function of frequency (Fig. 3E). The parameter D^*_{slow} was 0.19 (0.33 Hz), 0.38 (0.67 Hz), 0.29 (1.0 Hz) and 0.46 (2.0 Hz), and it increased approximately exponentially as a function of frequency (Fig. 3F).

Upon closer examination of the first few EPSPs in a train, it was often observed that after $EPSP_2$ there was a partial recovery in EPSP amplitude (Fig. 3A–D). This recovery is similar to that reported for the Mauthner fiber/giant fiber synapses in hatchetfish (Auerbach and Bennett, 1969) and may be a facilitation after $EPSP_2$, which is followed by the second component of depression.

Depression between $EPSP_1$ and $EPSP_2$ and response latency

To further investigate the abrupt change in kinetics we examined the latencies of the EPSPs in a train. Paired-pulse depression under conditions of depressed transmission at this synapse is associated with an increase in EPSP latency (Waldeck et al., 2000; Grove and Faber, 2008), which suggests that the kinetics of release are altered. Here, we analyzed the latencies of $EPSP_1$ and $EPSP_2$ when the M-axon was stimulated with trains of pulses delivered at 2 Hz, with an inter-train period of 60 s. Fig. 4A shows an example of normalized $EPSP_1$ and $EPSP_2$ (means of 8 traces), with latencies of 0.42 and 0.54 ms, respectively. $EPSP_1$ and $EPSP_2$ latencies averaged 0.57±0.10 ms (mean ± s.d.; N=162; 9 cells) and 0.68±0.17 ms (mean ± s.d.; N=128; 9 cells) and were statistically different (t-test P<0.0001). The cumulative histograms clearly show an increase in latency for $EPSP_2$, with a 50% shift of 0.08 ms (Fig. 4B). This increase may suggest a reduced release probability (Lin and Faber, 2002). It may indicate that the fast and slow components of depression are associated with relatively high and low release probabilities, respectively.

Recovery from depression

To investigate recovery from stimulus train-induced depression, we stimulated the M-axon with conditioning trains followed by a test stimulus (see Materials and methods). Fig. 5 illustrates an example in which amplitude and latency recovered exponentially with time constants of 17.9 and 16.6 s, respectively. On average, both the amplitude and latency of evoked EPSPs recovered exponentially with time constants of 16.1 and 13.2 s (95% confidence intervals: 12.49–22.55 and 9.13–22.44 s), respectively (Fig. 5D). A strong inverse correlation between the latency and amplitude of evoked EPSPs during recovery was observed (Fig. 5E). The similar recovery kinetics and the correlation between EPSP amplitude and latency suggest that the kinetics of release and the release probability during activity are related.

Effect of manipulating calcium on synaptic transmission and its dynamics

As Ca^{2+} is essential for release and is implicated in the modulation of short-term plasticity, we examined the effects of altering Ca^{2+} levels and dynamics on the initial level of release and the kinetics of depression. Specifically, we (1) chelated intracellular calcium ions presynaptically, (2) altered calcium influx by broadening the presynaptic action potentials, and (3) substituted Ba^{2+} for Ca^{2+} in

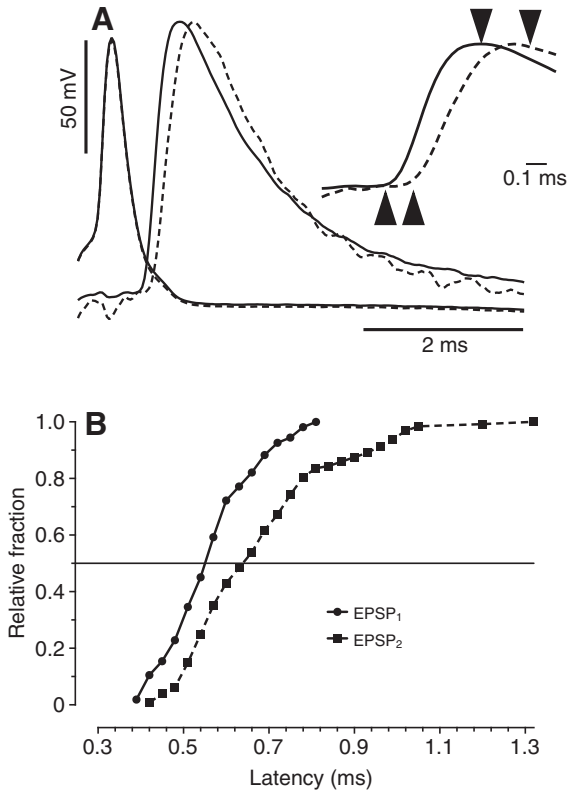

Fig. 4. Response latency. (A) An M-axon spike and an evoked EPSP (normalized) after the first (solid line) and the second (dashed line) stimulus. Inset depicts EPSPs on an expanded scale. Note the change in on-set (arrows) and peak (arrowheads) latencies. (B) Cumulative frequency distribution of $EPSP_1$ and $EPSP_2$ latencies. Relative fraction is the frequency of occurrence divided by the maximum frequency.

the extracellular medium. Because this *in vivo* preparation is inaccessible for Ca^{2+} imaging, our interpretations are partly based upon assumptions about the intracellular concentrations and distribution of Ca^{2+} ions.

Effect of BAPTA and EGTA

Using buffers with fast and slow forward rate constants also allowed us to probe the presynaptic organization of release sites. Therefore, we first determined the effect of the buffers on the amplitude of $EPSP_1$. Both BAPTA and EGTA were effective in reducing the amplitude of $EPSP_1$ (examples in Fig. 6Ai,Bi). The calcium buffers did not alter the amplitude or duration of the M-axon spikes (Fig. 6Aii,Bii), indicating the reduction in $EPSP_1$ amplitude was not the result of changes in the presynaptic waveform. Also, the reduction in the amplitude of $EPSP_1$ was not apparently due to the effect of the buffers on the time course of release after an action potential, given the almost invariant shape of the normalized EPSPs (Fig. 6Aiii,Biii). Therefore, asynchronous release is also unlikely. These results suggest that the buffers reduced the quantal content of release (Hochner et al., 1991). The buffer effect was concentration dependent (Fig. 6C); 10 mmol l^{-1} BAPTA or EGTA in the presynaptic electrode decreased the first EPSP amplitude by approximately 20% [fractional decrease (f.d.) was 0.24±0.06 and 0.22±0.03, respectively]. A tenfold increase in buffer concentration produced an approximately threefold increase in the effect (f.d., BAPTA 0.56±0.13, EGTA 0.52±0.07). In summary, the effects of the two buffers were similar despite the difference in their forward rate constants (Tsien, 1980).

Slow buffers, such as EGTA, could lower the basal level of calcium, which in turn could change the phosphorylation state of proteins involved in exocytosis and thus reduce EPSP amplitude. In other words, the reduction in EPSP amplitude may be due to a change in the biochemical properties of the terminal and not to a change in calcium dynamics. In addition, the calcium shift might be temporary, as activity could eventually restore the normal basal level. Nevertheless, to minimize basal fluctuations of calcium, some experiments were done in which the intracellular M-axon electrode had an EGTA solution buffered with calcium (see Materials and methods), which effectively clamps the calcium concentration in the pipette to 100 nmol l^{-1}. This solution had an intermediate effect (f.d. of 0.31±0.07; Fig. 6C). Because variability in buffer access to presynaptic terminals could not be controlled under the conditions of our experiments, we cannot make any quantitative conclusions based on the comparison of the effectiveness of different concentrations of BAPTA and EGTA. However, we can conclude that the two chelators reduced the amplitude of $EPSP_1$ to a similar degree.

We also tested the effect of chelating internal calcium on the depression induced by the low frequency trains of stimuli. The magnitude of the fast component of depression, D_{fast}, was significantly increased from 0.51±0.03, 0.32±0.12 and 0.47±0.04 to 0.68±0.03, 0.56±0.10 and 0.65±0.02 for 10 mmol l^{-1} BAPTA (N=3), 10 mmol l^{-1} EGTA (N=4) and 100 mmol l^{-1} 'buffered' EGTA (N=6), respectively (means ± s.e.m.; t-test P=0.0056, 0.0091 and 0.0017, respectively). The buffers also dramatically reduced the magnitude of the slow component of depression and slowed the

Table 1. Calcium buffer effect on the kinetics of depression

	10 mmol l^{-1} BAPTA (N=3)		10 mmol l^{-1} EGTA (N=4)		100 mmol l^{-1} EGTA (N=6)	
	Before	After	Before	After	Before	After
τ (s)	75.4	92.4	37.8	64.3	27.6	77.9
95% CI	60.4–100.3	54.3–309.9	32.7–44.8	38.3–197.9	24.1–32.2	58.4–117
D^*_{slow}	0.25	0.11	0.39	0.16	0.29	0.10
95% CI	0.23–0.27	0.08–0.13	0.37–0.41	0.12–0.20	0.26–0.31	0.09–0.11
F	126.3 (3,401)	183.0 (3,230)	115.10 (3,509)			
P	**<0.0001**	**<0.0001**	**<0.0001**			
R^2	0.78	0.36	0.93	0.61	0.77	0.50

Summary of the exponential fits to normalized, averaged data before and after injection of buffers. Fitting parameters (time constant τ and slow component of depression D^*_{slow}, see Results) are given with their 95% confidence intervals (CI). The final three rows of the table contain a statistical description of the exponential fits. The 'before' and 'after' curves were compared using an F-test; P-values indicate that the curves were statistically different. R^2 indicates the goodness-of-fit.

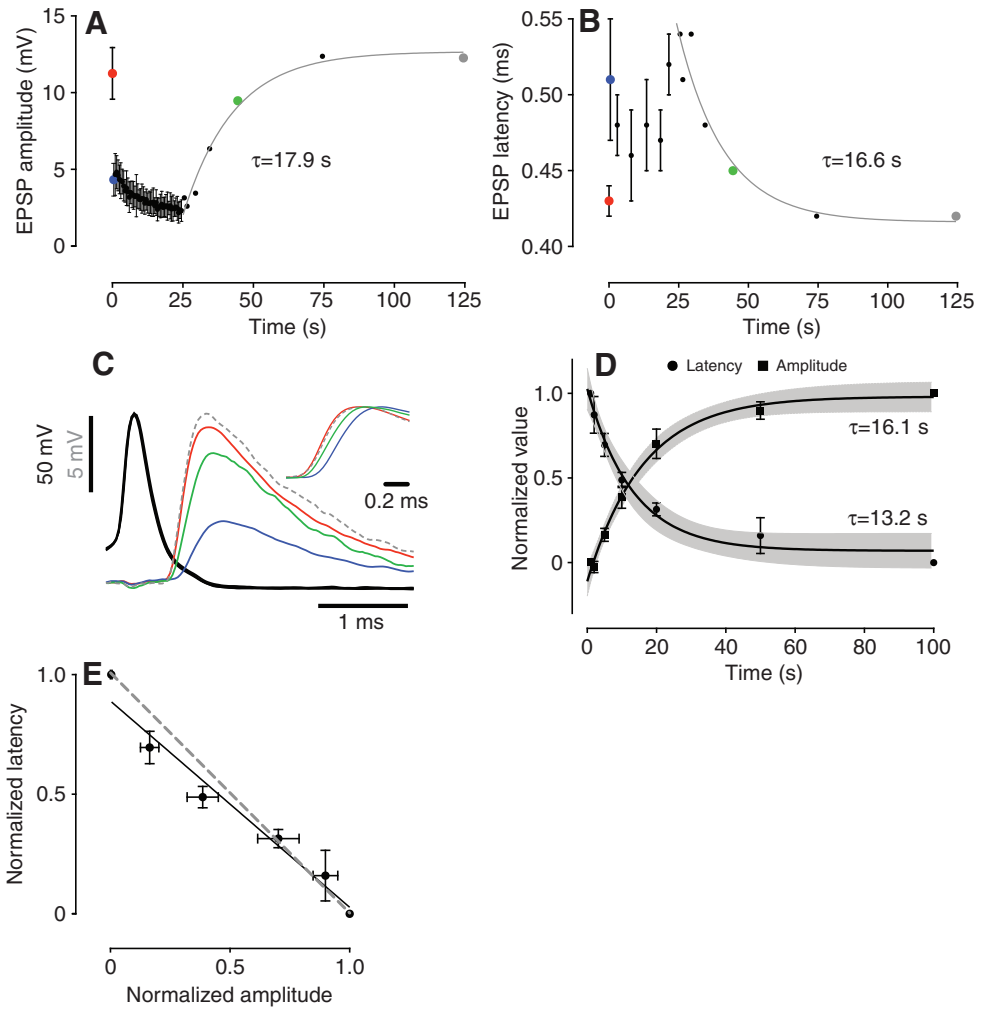

Fig. 5. Recovery from depression. (A) EPSP amplitudes from one standard recovery experiment (N=7 trains of stimuli; means ± s.d.). (B) EPSP latencies from the same experiment. The gray curves in A and B are exponential fits. (C) Superimposed M-axon and EPSP waveforms from the same experiment as in A and B (colors correspond to those in A and B). Inset depicts normalized EPSPs (note change in latency). (D) Normalized amplitude and latency recovery data (means ± s.e.m.; amplitude, N=9 pairs, latency, N=7 pairs; each data point for a pair represents the mean of several trains). The black curves are exponential fits. Gray-shaded areas represent 95% confidence bands. (E) Inverse correlation between normalized amplitude and latency from D. Black line represents a fitted linear function, y=–0.86x+0.89 (R^2=0.9691). The gray dashed line is y=1–x.

kinetics of its development. Parameters of the single-exponential functions (Eqn 1) fitted to the before and after data were statistically different (Table 1, Fig. 7A–C). D^*_{slow} decreased by 44, 41 and 34% with 10 mmol l^{-1} BAPTA, 10 mmol l^{-1} EGTA and 100 mmol l^{-1} 'buffered' EGTA, respectively. The time constant, τ, increased by 23, 70 and 82% from control values. These measurements indicate that treatment with buffers decreased evoked release, and increased the first and reduced the second component of depression, slowing the development of the latter.

Effect of presynaptic K$^+$-channel blockers

To further probe the properties of release and its depression at these synapses, we modified the influx of Ca^{2+} through Ca^{2+} channels by changing the waveform of the presynaptic action potentials. The repolarizing phase of the action potential is due to sodium conductance inactivation and an increase in potassium conductance (Hodgkin and Huxley, 1952). Blocking voltage-sensitive K^+ channels with TEA and 4-AP increases spike duration. Blocking these channels in the axon hillock initial segment prolongs M-axon spikes recorded in the soma (Kaars and Faber, 1981; Titmus and Faber, 1986). K^+-channel blockers (injected in the axon) also prolonged the M-cell spikes recorded in the axon, ~2.1–3.0 mm from the axon hillock (Fig. 8). Injection of TEA/4-AP did not change the M-cell resting membrane potential. The duration and, to a lesser degree, amplitude of the spike increased progressively as the number of injections increased. However, most of the increase in spike duration occurred at the later phase of the spike (Fig. 8, inset), reflecting the contribution of the more prolonged spike generated at the axon hillock initial segment. Prolonged injection led to the generation of multiple spikes activated by a single current pulse and antidromic doublets or triplets, presumably because the repolarization outlasted the refractory period. We did not analyze such data.

Surprisingly, these changes in the M-axon action potential duration were associated with a reduction in the amplitude of evoked EPSPs (Fig. 9). In the example shown in Fig. 9A, EPSP amplitudes were 5.01, 4.63 and 3.63 mV, and their peak derivatives (dV/dt) decreased from 16.59 to 16.05 and 12.26 mV ms^{-1} (Fig. 9Aii), indicating that transmitter release was reduced or became asynchronous. Asynchrony was also signaled by the broadening of the evoked EPSP peak accompanied by a fragmentation of the response (Fig. 9Aii). Changes in the EPSP amplitude and peak derivative were associated with the observed increase in presynaptic spike duration (Fig. 9Aiii) and a decrease in the M-spike repolarization rate (dV/dt; Fig. 9Aiv), i.e. with a broadened presynaptic spike. In this example, the half-widths of the illustrated M-spikes were 0.33, 0.39 and 0.48 ms and the derivative minima were –321.19, –261.38 and –193.85 mV ms^{-1}. On average, the M-spike parameters, 50% duration and dV/dt minimum, changed from 0.48±0.13 ms and –242.3±47.2 mV ms^{-1} to 0.65±0.16 ms and –171.8±33.7 mV ms^{-1} (paired t-test $P_{duration}$=0.0140 and $P_{dV/dt}$=0.0105), respectively. EPSP amplitude and dV/dt maximum

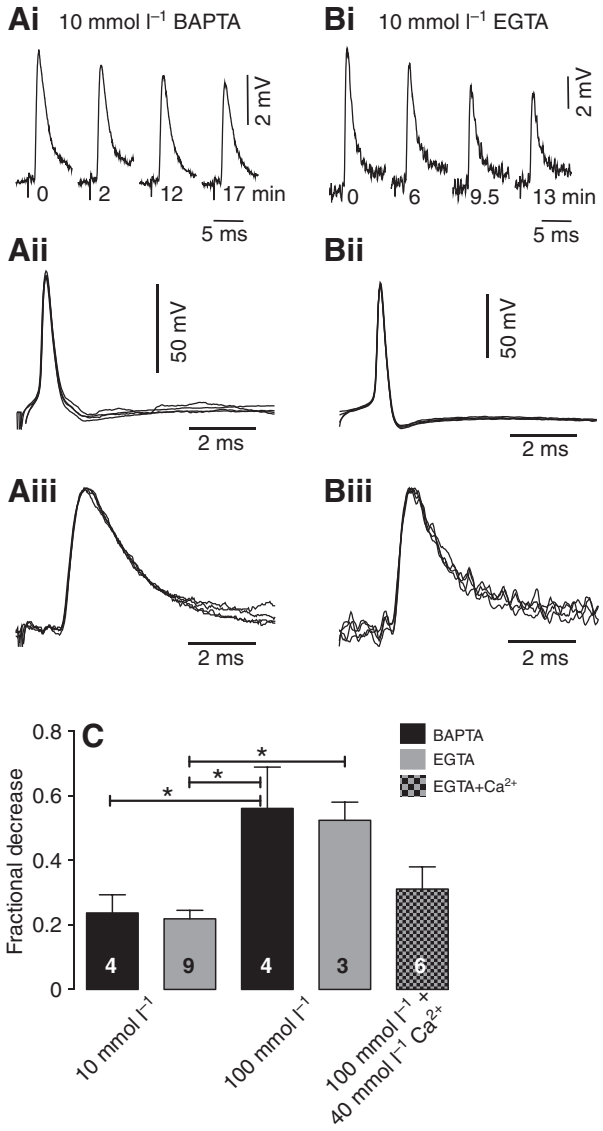

Fig. 6. Effect of Ca^{2+} buffers on $EPSP_1$. (Ai,Bi) An example showing the effect of 10 mmol l^{-1} BAPTA (Ai) and 10 mmol l^{-1} EGTA (Bi) on the EPSPs elicited by the first stimulus in the train. The recording time relative to control (0 min) is shown below the traces. (Aii,Bii) M-spikes corresponding to EPSPs in Ai and Bi. (Aiii,Biii) Normalized EPSPs (same data as in Ai,Bi). (C) Effect of different concentrations of BAPTA and EGTA on the fractional decrease in $EPSP_1$ (means + s.e.m.); fractional decrease is defined as $(EPSP_{1,control}–EPSP_{1,chelator})/EPSP_{1,control}$. Numbers inside the bars indicate the number of experiments (in each experiment EPSPs from several trains of stimuli at the same frequency were averaged). Asterisks denote significant difference (P<0.05) between pairs of treatments determined by one-factor ANOVA (P=0.0024) followed by Tukey's multiple comparison test.

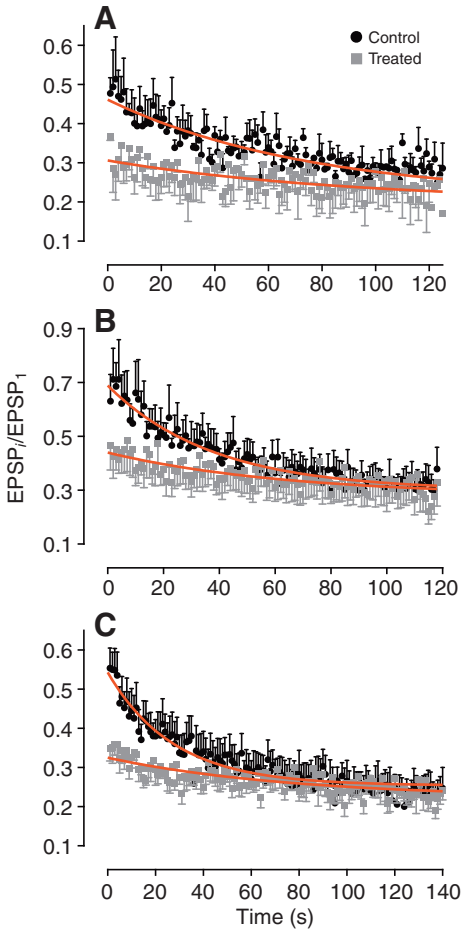

Fig. 7. Effect of Ca^{2+} buffers on the kinetics of depression. (A–C) Normalized data from three (10 mmol l^{-1} BAPTA, A), four (10 mmol l^{-1} EGTA, B) and six (100 mmol l^{-1} 'buffered' EGTA, C) experiments ($EPSP_1$ is omitted). Red curves are single exponential functions, fitted from $EPSP_2$ to $EPSP_{SS}$ (see Table 1 for statistical analysis).

changed from 6.9±1.1 mV and 29.4±6.7 mV ms^{-1} to 5.2±1.2 mV and 18.2±3.9 mV ms^{-1} (paired t-test $P_{amplitude}$=0.0059 and $P_{dV/dt}$=0.0204), respectively (Fig. 9Bi,Bii).

The effects of TEA/4-AP on the two components of depression were quantified as for the Ca^{2+} chelators. The amplitudes of $EPSP_1$, $EPSP_2$ and $EPSP_{SS}$ were all reduced. The magnitude of the fast component, D_{fast}, did not change significantly ($D_{fast,control}$=0.41±0.09 and $D_{fast,TEA/4AP}$=0.45±0.15; t-test P=0.2712; means ± s.e.m.; N=5 experiments). Fitting an exponential function (Eqn 1) into the before and after data (Fig. 9C, gray curves) showed that the magnitude of the slow component also did not change significantly; D^*_{slow} was 0.29 and 0.27 (95% confidence intervals: 0.28–0.30 and 0.25–0.30), respectively. However, the time constant of the development of the slow component was reduced, indicating that it developed faster, after the TEA/4-AP injection. The time constants were significantly different (34.5 and 12.9 s, respectively; 95% confidence intervals: 30.4–39.8 and 11.4–15.0 s, respectively; F-test: F=698.6, P<0.0001).

Effect of Ba^{2+} ions on release and kinetics of depression

Knowledge of the relative efficacies of divalent ions in triggering neurotransmitter release may give insight into the processes controlling exocytosis and the specificity of the native calcium sensor for release (Augustine and Eckert, 1984; Neves et al., 2001). Here we exchanged Ca^{2+} for Ba^{2+} in equimolar amounts to determine its effect on $EPSP_1$ and depression at the M-axon/CRN synapse. The barium effect, which initially was manifested as an increase in EPSP amplitude, began to occur within tens of seconds to minutes after the superfusion solutions were changed (Fig. 10A). During this and later periods of the experiment, the M-spike waveform did not change (Fig. 10B), indicating that Ba^{2+} ions had no effect on spike-generating mechanisms. However, Ba^{2+} had a pronounced effect on

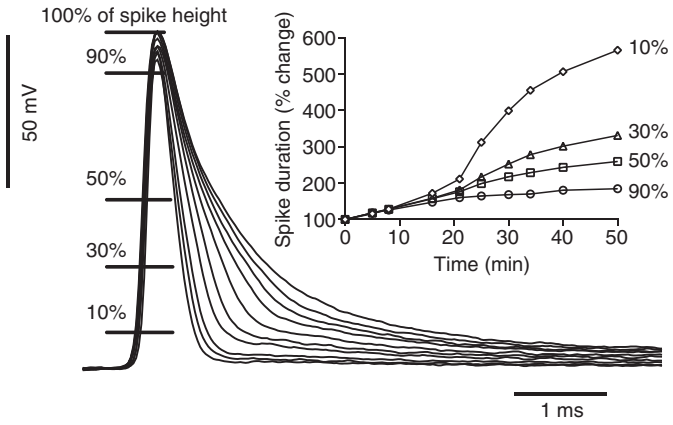

Fig. 8. Effect of K^+-channel blockers TEA and 4-AP on the M-spike duration. In this experiment each injection lasted for 1 min and was repeated after 1, 6, 9, 17, 22, 26, 31, 35, 41 and 51 min. Antidromically evoked M-spikes were recorded immediately before injection of K^+-channel blockers. The percentage change in spike duration at 10, 30, 50 and 90% of the spike height (marked by the horizontal lines) was calculated from these traces. Inset: the time course of the TEA/4-AP effect.

EPSP amplitude and kinetics. Ba^{2+} altered the time course of release, which was exhibited as a rightward shift in peak times and an increase in EPSP duration (Fig. 10B). The kinetics of short-term plasticity were also remarkably changed by Ba^{2+}. Barium treatment reduced D_{fast} from 0.79±0.03 to 0.47±0.16 (*t*-test P=0.0411). Additionally, the exponential fits to these data indicated that the time constants of the slow component of depression (τ_{slow}) in the calcium and barium solutions were 40.82 and 57.84 s (95% confidence intervals: 37.22–45.19 and 50.27–68.09 s), respectively, while $D^*_{slow(Ca)}$ and $D^*_{slow(Ba)}$ were 0.28 and 0.89 (95% confidence intervals: 0.27–0.29 and 0.84–0.95), respectively (F-test: F=334.6, P<0.0001). Interestingly, the presence of Ba^{2+} ions in the superfusate substantially increased delayed or asynchronous release (Fig. 10D). Such an increase has also been observed at the neuromuscular junction (Silinsky, 1978).

DISCUSSION

We have described properties of neurotransmitter release and kinetics of activity-dependent depression at the M-cell to CRN synapse stimulated at low frequencies. The results indicate that the time course of activity-dependent plasticity could be ascribed to a two-component depression, with a first component that develops rapidly and is relatively long lasting and a second component that develops one or two orders of magnitude slower. Depression was associated with an increased latency of synaptic transmission, suggesting multiple changes in the release properties following the first response. Moreover, the kinetics of depression depended on intracellular calcium, suggesting that processes which alter intracellular calcium dynamics could modulate depression at the M-cell/CRN synapse.

Release in the absence of depression, as measured by the amplitude of $EPSP_1$, exhibited unusual properties. First, BAPTA and EGTA were similarly effective in reducing release. Second, broadening the action potentials with K^+-channel blockers decreased $EPSP_1$. Third, release was more sensitive to Ba^{2+} than to Ca^{2+} and was enhanced by Ba^{2+}. We have not found systematic differences in these properties between different functional and morphological classes of CRNs, classified on the basis of the EPSP decay and on CRN axonal arborization patterns (Grove et al., 2011). However, we do not eliminate the possibility that some properties of depression are different among the heterogeneous group of CRNs.

We first discuss the organization of release sites at this synapse, then the anomalous results that distinguish this synapse from others that have been studied extensively. Finally, we consider the possibility that the two-component depression reflects the unique requirements for this synaptic connection.

Ca^{2+} domains and release

Exogenous calcium buffers with fast (BAPTA) and slow (EGTA) binding kinetics are used to probe the coupling between calcium channels and transmitter release (reviewed in Augustine, 2001). At the squid giant synapse (Adler et al., 1991) and mammalian cortical GABAergic synapses (Bucurenciu et al., 2010), BAPTA, but not EGTA, is effective in reducing transmission, suggesting that calcium channels are tightly coupled to the release sensor and that calcium domains do not overlap. However, at young calyces of Held (Borst and Sakmann, 1996), terminals of rat cortical pyramidal cells (Ohana and Sakmann, 1998; Rozov et al., 2001), and connections between rat cerebellar granule cells and stellate cells (Chen and Regehr, 1999), millimolar concentrations of EGTA reduce release, suggesting that many calcium channels contribute to the release of a single vesicle. Release at the M-axon/CRN synapse was also sensitive to millimolar concentrations of EGTA in the intracellular pipette. Although we cannot specify the intracellular EGTA concentration, this result suggests that Ca^{2+} channels in these terminals are loosely coupled to the Ca^{2+} sensor for exocytosis and that possibly many channels cooperate in the release of a single vesicle. Such a 'microdomain' organization of the release sites may decrease synaptic noise due to stochastic kinetic behavior of single channels and also provide a high safety factor for evoked release (Stanley, 1997), which is functionally important for the M-cell network. While it is difficult to explain the apparent equivalent potency of BAPTA and EGTA, the observation that they have qualitatively similar actions still supports this conclusion.

Anomalous effect of K^+-channel blockers

Our results indicate an anomalous relationship between the release of neurotransmitter and duration of the M-cell spike. The two measures of exocytosis that we used, EPSP amplitude and its maximum derivative, indicate that release magnitude is negatively correlated with spike duration, at least in the examined range. Similarly, in the nervous system of jellyfish, an increase in motor neuron spike duration leads to a reduction in the size of the muscle excitatory potentials, because of a reduction in the peak presynaptic Ca^{2+} current (Spencer et al., 1989). Also, a similar effect was observed at the zebrafish neuromuscular junction (Wen and Brehm, 2005). However, in other preparations, including the squid giant synapse (Augustine, 1990), rat granule to Purkinje cell synapse (Sabatini and Regehr, 1997), sensory neurons of *Aplysia* (Hochner et al., 1986) and crayfish neuromuscular junction (Lin and Faber, 2002), spike broadening enhances release.

A negative correlation between spike duration and EPSP amplitude may be explained by assuming less calcium flowed into the presynaptic terminal under the conditions of our experiments. Ca^{2+} conductance may reach its maximum, but calcium influx is relatively small at the peak of depolarization because the inward driving force is minimal. During a fast repolarization, the inward driving force on Ca^{2+} develops quickly, producing a brief, large calcium current. Blocking voltage-sensitive K^+ channels slows the repolarization phase, which

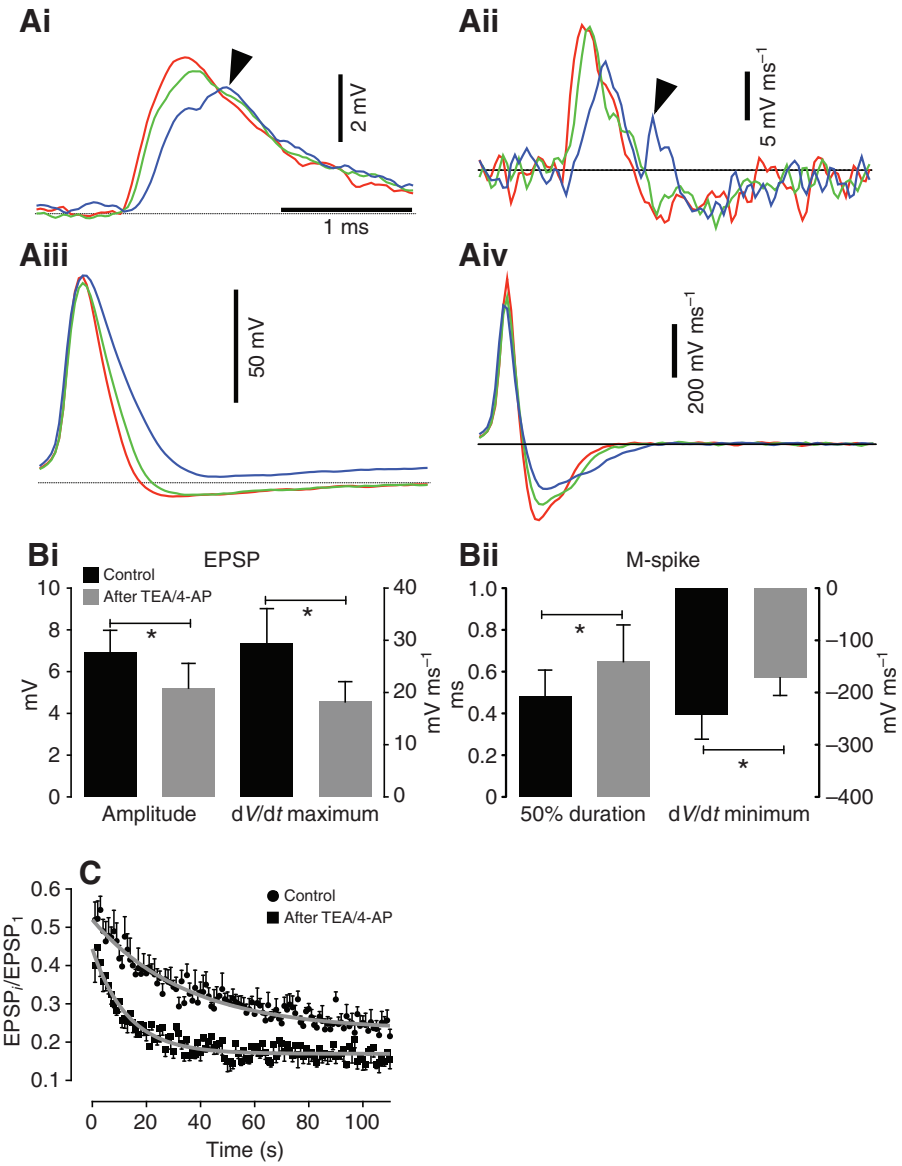

Fig. 9. Effect of K^+-channel blockers on release and depression. (Ai) EPSPs elicited by the first M-axon spike in three episodes of stimulation followed by 1 min of iontophoretic injection of TEA/4-AP (red, green and blue, corresponding to the first, second and third episodes, 0, 5 and 16 min after the onset of the recording session, respectively). (Aii) Derivatives of the EPSP traces in Ai. EPSP in blue has a second peak (arrowhead). (Aiii,Aiv) Superimposed M-spikes and their derivatives from the same episodes as in Ai. M-spikes became broader (Aiii) and the repolarization was slower (Aiv; smaller negative peaks) after each injection. Time scale is the same in Ai–Aiv. (Bi,Bii) The different parameters of EPSPs and M-spikes (means ± s.e.m.; N=5 pairs from the same number of experiments; up to 10 trains in each experiment) before (black) and after (gray) iontophoresis of TEA/4-AP. (Bi) EPSP amplitudes (left y-axis) and maximum EPSP derivatives (right y-axis) decreased with treatment (paired t-test $P_{amplitude}$=0.0059 and $P_{dV/dt}$=0.0204). (Bii) M-spike duration at the 50% spike height (left y-axis) and minimum M-spike derivatives (right y-axis) also changed (paired t-test $P_{duration}$=0.0140 and $P_{dV/dt}$=0.0105). (C) Blocking voltage-sensitive K^+ conductance alters the kinetics of depression. Normalized data (means ± s.e.m.; N=5 pairs from the same number of experiments; several trains were averaged in each experiment; $EPSP_1$ is omitted) before and after treatment. Gray curves are single exponential functions (Eqn 1), fitted from $EPSP_2$ to $EPSP_{SS}$.

decreases the rate of development of the calcium driving force, leading to a smaller peak calcium current. However, in other systems the integral of the Ca^{2+} current is more directly related to release and increases with spike broadening (Llinas et al., 1981; Augustine, 1990). Possibly, in the case of the M-cell/CRN synapse, as well as the jellyfish and zebrafish neuromuscular junctions, the calcium channels have much faster opening/closing kinetics, and release is more dependent on the peak calcium current than on its integral. This notion is consistent with the observation that the latency of transmitter release at the M-axon to CRN synapses is shorter than at other synapses (Sabatini and Regehr, 1999).

Barium effect

We show here that Ba^{2+} enhanced transmission, as opposed to its effect in other systems, including the neuromuscular junction (Zengel and Magleby, 1977), the superior cervical ganglion synapses (Zengel et al., 1980) and squid giant synapse (Augustine and Eckert, 1984), where the response to a single stimulus was reduced. Barium also slowed the kinetics of depression. The mechanisms underlying these effects are not clear. They may include an enhanced Ba^{2+} current through the presynaptic Ca^{2+} channels or the postsynaptic nicotinic, acetylcholine-gated channels or a greater affinity of the Ca^{2+} sensor for Ba^{2+}. However, results from the other systems are not consistent with either enhanced current or greater affinity for Ba^{2+} (Brigant and Mallart, 1982; Augustine and Eckert, 1984; Neves et al., 2001; Maeda et al., 2009). Additional mechanisms may involve indirect actions of Ba^{2+}; for example, by increasing $[Ca^{2+}]_i$. The Ba^{2+}-induced enhancement at this synapse points to an unusual intrinsic property of release that contrasts with that at other synapses.

EPSP amplitude depression and latency

Although fluctuations in the latency of the postsynaptic responses are sometimes considered random, they can instead reflect changes in the release probability and may be correlated with PSP amplitude (Lin and Faber, 2002; Boudkkazi et al., 2007). Previous work showed that the paired-pulse protocol, under conditions of steady-state depression, revealed that responses to the second pulse have longer latencies (Waldeck et al., 2000). Latencies of the steady-state responses to prolonged stimulus trains were also found to increase with stimulation frequency (Grove and Faber, 2008). We show here that the negative correlation between latency and

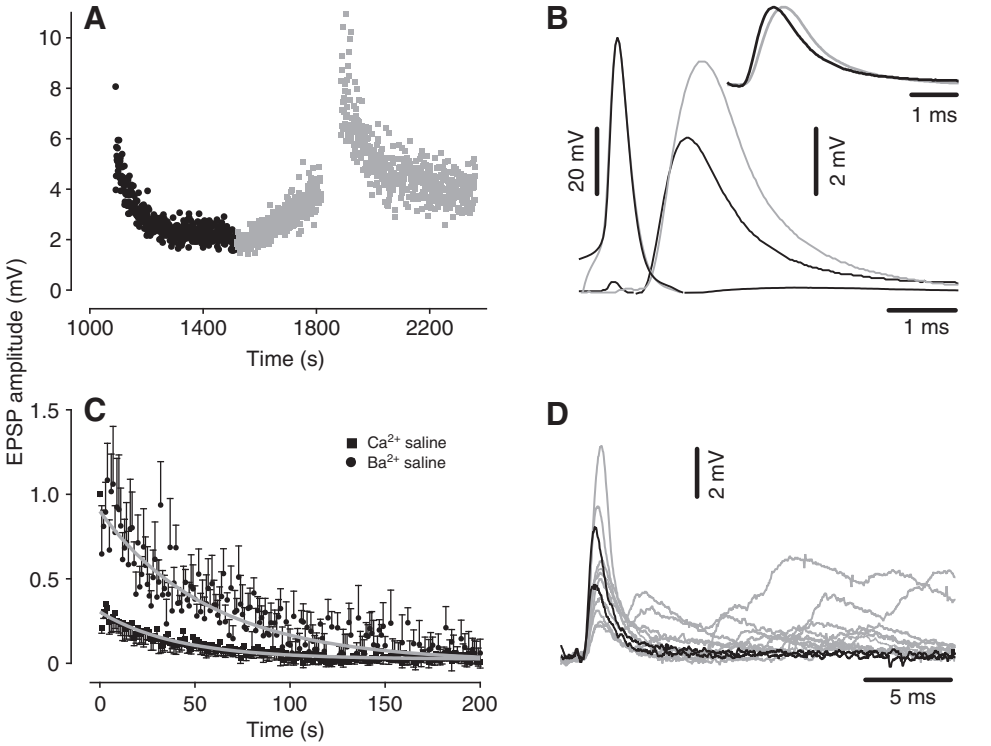

Fig. 10. (A) An example of activity-dependent depression of EPSP amplitude (1 Hz stimulation frequency; black and gray represent control and Ba^{2+}-containing superfusing solutions; the same colors are used in all panels). (B) Superimposed M-spikes and EPSPs in Ca^{2+}- and Ba^{2+}-containing saline, from the same experiment. Inset: normalized EPSPs. (C) Ba^{2+}-induced enhancement effect and change in the kinetics of depression (means ± s.e.m.; N=5 pairs from the same number of experiments; several trains were averaged in each experiment). In each experiment up to five episodes of stimulation before and during barium superfusion were averaged, scaled by the mean amplitude of the last 20 EPSPs, and normalized by the maximum EPSP amplitude. Gray curves are single exponential functions (Eqn 1), fitted from $EPSP_2$ to $EPSP_{SS}$. (D) Asynchronous or delayed release during Ba^{2+}-containing saline superfusion. Control and Ba^{2+} traces are superimposed (note the stronger release after the evoked EPSP in Ba^{2+}).

amplitude also holds true under conditions of maximal initial release probability and low-frequency stimulation (see Grove and Faber, 2008). The mechanism of such latency changes may involve changes in the state of the exocytotic machinery; for example, a shift in the properties of a Ca^{2+} sensor (Hsu et al., 1996). Alternatively, a change in the spatial distribution of the effective $[Ca^{2+}]$ at individual release sites could result in the increased latency, especially as our results with BAPTA and EGTA suggest a dependency of release on overlapping domains.

Kinetics of depression

Synapses exhibit a great diversity in the sign and kinetics of activity-dependent plasticity. They may be depressing or enhancing, or show enhancement followed by depression, with time constants of these processes spanning several orders of magnitude. Commonly, at depressing synapses, stimulus trains elicit depression that proceeds with a mono-exponential time course. Examples of such synapses include the calyx of Held in the rat brainstem (von Gersdorff et al., 1997), pyramidal cell synapses in rat primary visual cortex (Abbott et al., 1997), excitatory synapses in layer 4 of rat somatosensory cortex (Petersen, 2002), inhibitory synapses in mouse hippocampus CA3 region (Szabó et al., 2010), and a subset of lamprey spinal synapses (Parker, 2003). Less commonly, train stimuli elicit depression with a more complex time course. Some connections between cortical layers 2/3 and 5 exhibit a double-exponential time course of frequency-dependent depression (Williams and Atkinson, 2007). We showed here that the kinetics of EPSP amplitude depression at the M-cell/CRN synapse were complex, with at least two time constants. In contrast, recovery from depression followed mono-exponential kinetics. The discrepancy between depression and recovery kinetics is difficult to explain; however, this finding points to another unusual and interesting feature of this connection. Additionally, kinetics may be influenced by the presence of facilitation, as evidenced by an increase in EPSP amplitude after $EPSP_2$.

Functional significance

Excitation of one M-cell is necessary and sufficient for the production of the stereotyped escape behavior. The M-cell network operates with a high safety factor for transmission of the first M-spike. Yet, in a number of organisms, including goldfish (Korn and Faber, 2005), hatchetfish (Aljure et al., 1980) and butterfly fish (Starosciak et al., 2008), repetition of the M-cell-mediated escape response is suppressed for several seconds. Multiple mechanisms provide a safeguard against repetitive movements. First, excitation of the M-cell on one side will also inhibit the contralateral M-cell through a pathway involving activation of CRNs (Korn and Faber, 2005). Second, there is also a feedforward inhibition of the M-cell. Finally, a powerful depression of the M-cell/CRN synapse, which relays excitation to motor neurons at the supraspinal level, also contributes to guaranteeing a single escape in the face of continued excitatory drive to the M-cell. The long-lasting depression might also guard against subsequent CRN excitation by combined inputs from the M-axon and other cells comprising the brainstem escape network (Gahtan et al., 2002). While it is also tempting to suggest this depression contributes to habituation of the escape response (Aljure et al., 1980), the locus of this form of behavioral plasticity is more likely to be at the level of the afferent inputs to the M-cell. Regardless, the mechanistic properties of depression at these junctions mirror the behavioral requirements; namely, for a single escape movement that can be succeeded by purposeful swimming activity.

ACKNOWLEDGEMENTS

We thank Drs Kamran Khodakhah, Alberto Pereda (AECOM), Thomas Preuss (Hunter College, CUNY) and Jen-Wei Lin (Boston University) for discussions and help. We thank Maurice Volaski for computer assistance. Support was provided by NIH training grant T32NS007439. Deposited in PMC for release after 12 months.

REFERENCES

Abbott, L. F., Varela, J. A., Sen, K. and Nelson, S. B. (1997). Synaptic depression and cortical gain control. *Science* **275**, 220-224.

Adler, E. M., Augustine, G. J., Duffy, S. N. and Charlton, M. P. (1991). Alien intracellular calcium chelators attenuate neurotransmitter release at the squid giant synapse. *J. Neurosci.* **11**, 1496-1507.
Aljure, E., Day, J. W. and Bennett, M. V. (1980). Postsynaptic depression of Mauthner cell-mediated startle reflex, a possible contributor to habituation. *Brain Res.* **188**, 261-268.
Auerbach, A. A. and Bennett, M. V. (1969). Chemically mediated transmission at a giant fiber synapse in the central nervous system of a vertebrate. *J. Gen. Physiol.* **53**, 183-210.
Augustine, G. J. (1990). Regulation of transmitter release at the squid giant synapse by presynaptic delayed rectifier potassium current. *J. Physiol.* **431**, 343-364.
Augustine, G. J. (2001). How does calcium trigger neurotransmitter release? *Curr. Opin. Neurobiol.* **11**, 320-326.
Augustine, G. J. and Eckert, R. (1984). Divalent cations differentially support transmitter release at the squid giant synapse. *J. Physiol.* **346**, 257-271.
Betz, W. J. (1970). Depression of transmitter release at the neuromuscular junction of the frog. *J. Physiol.* **206**, 629-644.
Borst, J. G. and Sakmann, B. (1996). Calcium influx and transmitter release in a fast CNS synapse. *Nature* **383**, 431-434.
Boudkkazi, S., Carlier, E., Ankri, N., Caillard, O., Giraud, P., Fronzaroli-Molinieres, L. and Debanne, D. (2007). Release-dependent variations in synaptic latency: a putative code for short- and long-term synaptic dynamics. *Neuron* **56**, 1048-1060.
Brigant, J. L. and Mallart, A. (1982). Presynaptic currents in mouse motor endings. *J. Physiol.* **333**, 619-636.
Bucurenciu, I., Bischofberger, J. and Jonas, P. (2010). A small number of open Ca^{2+} channels trigger transmitter release at a central GABAergic synapse. *Nat. Neurosci.* **13**, 19-21.
Castellucci, V. F. and Kandel, E. R. (1974). A quantal analysis of the synaptic depression underlying habituation of the gill-withdrawal reflex in *Aplysia*. *Proc. Natl. Acad. Sci. USA* **71**, 5004-5008.
Chen, C. and Regehr, W. G. (1999). Contributions of residual calcium to fast synaptic transmission. *J. Neurosci.* **19**, 6257-6266.
Connors, B. W. and Prince, D. A. (1982). Effects of local anesthetic QX-314 on the membrane properties of hippocampal pyramidal neurons. *J. Pharmacol. Exp. Ther.* **220**, 476-481.
Faber, D. S. and Korn, H. (1978). Electrophysiology of the Mauthner cell: basic properties, synaptic mechanisms and associated networks. In *Neurobiology of the Mauthner Cell* (ed. D. S. Faber and H. Korn), pp. 47-131. New York: Raven Press.
Fortune, E. S. and Rose, G. J. (2000). Short-term synaptic plasticity contributes to the temporal filtering of electrosensory information. *J. Neurosci.* **20**, 7122-7130.
Funch, P. G., Wood, M. R. and Faber, D. S. (1984). Localization of active sites along the myelinated goldfish Mauthner axon: morphological and pharmacological evidence for saltatory conduction. *J. Neurosci.* **4**, 2397-2409.
Gahtan, E., Sankrithi, N., Campos, J. B. and O'Malley, D. M. (2002). Evidence for a widespread brain stem escape network in larval zebrafish. *J. Neurophysiol.* **87**, 608-614.
Garcia-Perez, E., Lo, D. C. and Wesseling, J. F. (2008). Kinetic isolation of a slowly recovering component of short-term depression during exhaustive use at excitatory hippocampal synapses. *J. Neurophysiol.* **100**, 781-795.
Grove, C. L. (2008). Fast synaptic transmission and heterogeneity in release probability in the vertebrate CNS mediated by multiple nicotinic receptors. PhD thesis, Albert Einstein College of Medicine, New York, NY, USA.
Grove, C. L. and Faber, D. S. (2008). Heterogeneity in release dynamics and release probability at a nicotinic CNS connection. *Soc. Neurosci. Abstr.* 432.18.
Grove, C. L., Szabo, T. M., McIntosh, J. M., Do, S. C., Waldeck, R. F. and Faber, D. S. (2011). Fast synaptic transmission in the goldfish CNS mediated by multiple nicotinic receptors. *J. Physiol.* **589**, 575-595.
Hackett, J. T. and Faber, D. S. (1983). Mauthner axon networks mediating supraspinal components of the startle response in the goldfish. *Neuroscience* **8**, 317-331.
Hackett, J. T., Cochran, S. L. and Greenfield, L. J., Jr (1989). Quantal transmission at Mauthner axon target synapses in the goldfish brainstem. *Neuroscience* **32**, 49-64.
Hochner, B., Klein, M., Schacher, S. and Kandel, E. R. (1986). Action-potential duration and the modulation of transmitter release from the sensory neurons of *Aplysia* in presynaptic facilitation and behavioral sensitization. *Proc. Natl. Acad. Sci. USA* **83**, 8410-8414.
Hochner, B., Parnas, H. and Parnas, I. (1991). Effects of intra-axonal injection of Ca^{2+} buffers on evoked release and on facilitation in the crayfish neuromuscular junction. *Neurosci. Lett.* **125**, 215-218.
Hodgkin, A. L. and Huxley, A. F. (1952). The components of membrane conductance in the giant axon of *Loligo*. *J. Physiol.* **116**, 473-496.
Hsu, S. F., Augustine, G. J. and Jackson, M. B. (1996). Adaptation of Ca^{2+}-triggered exocytosis in presynaptic terminals. *Neuron* **17**, 501-512.
Kaars, C. and Faber, D. S. (1981). Myelinated central vertebrate axon lacks voltage-sensitive potassium conductance. *Science* **212**, 1063-1065.
Kalkstein, J. M. and Magleby, K. L. (2004). Augmentation increases vesicular release probability in the presence of masking depression at the frog neuromuscular junction. *J. Neurosci.* **24**, 11391-11403.
Kandel, E. R., Schwartz, J. H. and Jessell, T. M. (2000). *Principles of Neural Science*. New York: McGraw-Hill.
Korn, H. and Faber, D. S. (2005). The Mauthner cell half a century later: a neurobiological model for decision-making? *Neuron* **47**, 13-28.
Lin, J. W. and Faber, D. S. (2002). Modulation of synaptic delay during synaptic plasticity. *Trends Neurosci.* **25**, 449-455.
Llinas, R., Steinberg, I. Z. and Walton, K. (1981). Presynaptic calcium currents in squid giant synapse. *Biophys. J.* **33**, 289-321.
MacLeod, K. M., Horiuchi, T. K. and Carr, C. E. (2007). A role for short-term synaptic facilitation and depression in the processing of intensity information in the auditory brain stem. *J. Neurophysiol.* **97**, 2863-2874.
Maeda, M., Tanaka, E., Shoudai, K., Nonaka, K., Murayama, N., Ito, Y. and Akaike, N. (2009). Differential effects of divalent cations on spontaneous and evoked glycine release from spinal interneurons. *J. Neurophysiol.* **101**, 1103-1113.
Neves, G., Neef, A. and Lagnado, L. (2001). The actions of barium and strontium on exocytosis and endocytosis in the synaptic terminal of goldfish bipolar cells. *J. Physiol.* **535**, 809-824.
Ohana, O. and Sakmann, B. (1998). Transmitter release modulation in nerve terminals of rat neocortical pyramidal cells by intracellular calcium buffers. *J. Physiol.* **513**, 135-148.
Parker, D. (2003). Variable properties in a single class of excitatory spinal synapse. *J. Neurosci.* **23**, 3154-3163.
Patton, C., Thompson, S. and Epel, D. (2004). Some precautions in using chelators to buffer metals in biological solutions. *Cell Calcium* **35**, 427-431.
Petersen, C. C. H. (2002). Short-term dynamics of synaptic transmission within the excitatory neuronal network of rat layer 4 barrel cortex. *J. Neurophysiol.* **87**, 2904-2914.
Rozov, A., Burnashev, N., Sakmann, B. and Neher, E. (2001). Transmitter release modulation by intracellular Ca^{2+} buffers in facilitating and depressing nerve terminals of pyramidal cells in layer 2/3 of the rat neocortex indicates a target cell-specific difference in presynaptic calcium dynamics. *J. Physiol.* **531**, 807-826.
Sabatini, B. L. and Regehr, W. G. (1997). Control of neurotransmitter release by presynaptic waveform at the granule cell to purkinje cell synapse. *J. Neurosci.* **17**, 3425-3435.
Sabatini, B. L. and Regehr, W. G. (1999). Timing of synaptic transmission. *Annu. Rev. Physiol.* **61**, 521-542.
Silinsky, E. M. (1978). On the role of barium in supporting the asynchronous release of acetylcholine quanta by motor nerve impulses. *J. Physiol.* **274**, 157-171.
Spencer, A. N., Przysiezniak, J., Acosta-Urquidi, J. and Basarsky, T. A. (1989). Presynaptic spike broadening reduces junctional potential amplitude. *Nature* **340**, 636-638.
Stanley, E. F. (1997). The calcium channel and the organization of the presynaptic transmitter release face. *Trends Neurosci.* **20**, 404-409.
Starosciak, A. K., Kalola, R. P., Perkins, K. P., Riley, J. A. and Saidel, W. M. (2008). Fast and singular muscle responses initiate the startle response of *Pantodon buchholzi* (Osteoglossomorpha). *Brain Behav. Evol.* **71**, 100-114.
Stevens, C. F. and Wesseling, J. F. (1999). Identification of a novel process limiting the rate of synaptic vesicle cycling at hippocampal synapses. *Neuron* **24**, 1017-1028.
Strichartz, G. R. (1973). The inhibition of sodium currents in myelinated nerve by quaternary derivatives of lidocaine. *J. Gen. Physiol.* **62**, 37-57.
Szabó, G. G., Holderith, N., Gulyás, A. I., Freund, T. F. and Hájos, N. (2010). Distinct synaptic properties of perisomatic inhibitory cell types and their different modulation by cholinergic receptor activation in the ca3 region of the mouse hippocampus. *Eur. J. Neurosci.* **31**, 2234-2246.
Szabó, T. M., Weiss, S. A., Faber, D. S. and Preuss, T. (2006). Representation of auditory signals in the M-cell: role of electrical synapses. *J. Neurophysiol.* **95**, 2617-2629.
Titmus, M. J. and Faber, D. S. (1986). Altered excitability of goldfish Mauthner cell following axotomy. I. Localization and ionic basis. *J. Neurophysiol.* **55**, 1440-1454.
Tsien, R. Y. (1980). New calcium indicators and buffers with high selectivity against magnesium and protons: Design, synthesis, and properties of prototype structures. *Biochemistry* **19**, 2396-2404.
von Gersdorff, H., Schneggenburger, R., Weis, S. and Neher, E. (1997). Presynaptic depression at a Calyx synapse: the small contribution of metabotropic glutamate receptors. *J. Neurosci.* **17**, 8137-8146.
Waldeck, R. F., Pereda, A. and Faber, D. S. (2000). Properties and plasticity of paired-pulse depression at a central synapse. *J. Neurosci.* **20**, 5312-5320.
Wen, H. and Brehm, P. (2005). Paired motor neuron-muscle recordings in zebrafish test the receptor blockade model for shaping synaptic current. *J. Neurosci.* **25**, 8104-8111.
Williams, S. R. and Atkinson, S. E. (2007). Pathway-specific use-dependent dynamics of excitatory synaptic transmission in rat intracortical circuits. *J. Physiol.* **585**, 759-777.
Zengel, J. E. and Magleby, K. L. (1977). Transmitter release during repetitive stimulation: selective changes produced by Sr^{2+} and Ba^{2+}. *Science* **197**, 67-69.
Zengel, J. E., Magleby, K. L., Horn, J. P., McAfee, D. A. and Yarowsky, P. J. (1980). Facilitation, augmentation, and potentiation of synaptic transmission at the superior cervical ganglion of the rabbit. *J. Gen. Physiol.* **76**, 213-231.